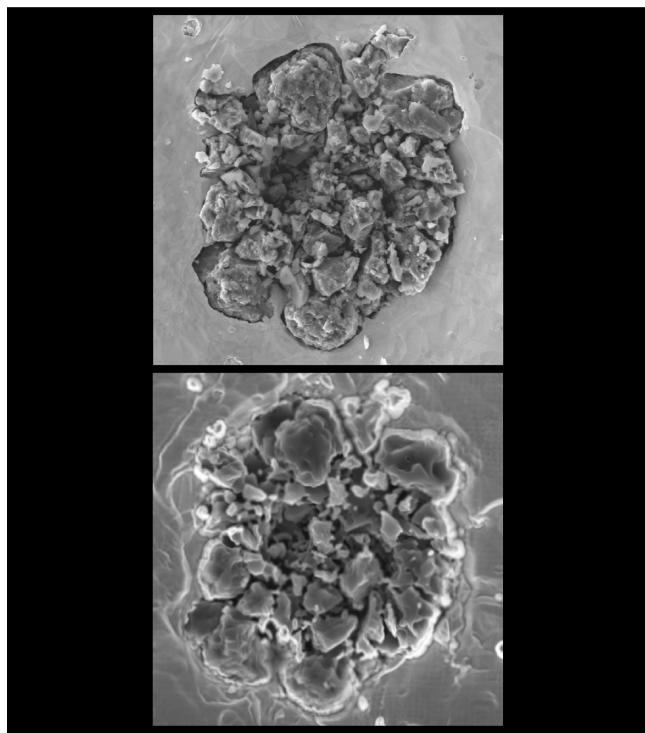


Laboratory Analysis of Stardust

Tiny dust grains extracted from primitive meteorites are identified to have originated in the atmospheres of stars on the basis of their anomalous isotopic compositions. Although isotopic analysis with the ion microprobe plays a major role in the laboratory analysis of these stardust grains, many other microanalytical techniques are applied to extract the maximum amount of information.

Ernst Zinner*

Laboratory for Space Sciences and the Physics Department, Washington University, One Brookings Drive, St. Louis, Missouri 63130, United States



In the 1950s, it has been firmly established that carbon and all heavier elements are produced in stars by stellar nucleosynthesis with a range of isotopic ratios.^{1,2} Although many stellar sources contributed material to the solar system, this material had been thoroughly homogenized during solar system formation, resulting in very uniform isotopic ratios throughout (planets, moons, asteroids, meteorites, interplanetary dust). As a consequence, isotopic signatures of individual stars were thought to have been completely obliterated. The abundances of elements and isotopes in the solar system were considered to represent only an average of many distinct stellar sources. This situation changed dramatically in 1987 with the discovery that primitive meteorites contain tiny grains of pristine stardust.^{3,4} The presolar, stellar origin of these grains is indicated by their unusual (“exotic”) isotopic compositions, which are completely different from that of the solar system. They must have condensed in the outflows of evolved stars and in supernova ejecta, survived interstellar travel and solar system formation, and were preserved in certain types of meteorites. In spite of their small size, they can be located in and extracted from their

meteoritic hosts and studied in detail in the laboratory. Because a given grain is a piece of a star, it can provide information on stellar evolution and nucleosynthesis, galactic chemical evolution, physical conditions in stellar atmospheres, dust processing in the interstellar medium, and conditions during solar system formation. Since the discovery of the first presolar grains, their study has grown into a new kind of astronomy, complementing traditional astronomical observations.^{5–7} The sophisticated analytical techniques that are used to study these precious grains are the focus of this paper.

■ ISOLATION OF PRESOLAR GRAINS

The first hints of the survival of presolar signatures in solar system materials came from isotopic anomalies found in meteorites, i.e., isotopic ratios different from those dominating the solar system, of the noble gases Ne and Xe. These hints were largely ignored and it was not until the discovery of anomalies in O, a major rock-forming element,⁸ that the idea of survival of presolar material in primitive meteorites was taken seriously. However, it turned out that the solids exhibiting isotopic anomalies in O (and, as it was later found out, in many other elements) had formed in the solar system and only inherited presolar signatures from their precursors. It took more than a decade to find *bona fide* stardust that had condensed in stellar environments. This feat was achieved by Prof. Ed Anders and his colleagues at the University of Chicago by “burning down the haystack to find the needle”.⁹ In this approach, chemical dissolution and physical separation techniques were used to track the carrier phases of isotopically anomalous “exotic” noble gas components, and this finally led to the separation of presolar diamond,⁴ silicon carbide (SiC),³ and graphite.¹⁰ These phases are not only high-temperature phases that must have had a condensation origin but are also chemically resistant and thus could be isolated by harsh chemical treatment. Once the grains were known to be present in meteorites, techniques were developed to locate and study them in situ without the chemical treatment, as discussed below.

■ TYPES OF PRESOLAR GRAINS

In spite of the grains’ low abundance and their small size, an ever increasing number of different types of presolar minerals have been identified. Table 1 lists presolar grain types, their

Published: December 11, 2012

Table 1. Presolar Grain Types Found in Primitive Meteorites

grain type	abundance ^a (ppm)	fraction (%)	size (μm)	stellar sources ^b
diamond	1400		0.002	SNe, solar system?
silicates	200		≤ 0.5	RGB, AGB, SNe
oxides	50		0.1–2	RGB, AGB, SNe, novae
SiC	30		0.2–50	
mainstream		90		AGB
type AB		4–5		J stars?
type X		1		SNe
types Y and Z		up to 6		low metallicity AGB
type C		0.1		SNe
nova		0.1		novae
graphite	2		1–20	SNe, AGB, born-again AGB
Si nitride	0.002		≤ 1	SNe
TiC	~ 0.001		0.01–0.5	SNe, AGB

^aAbundances (in parts per million) vary with meteorite type. Shown here are maximum values. ^bSNe: Core collapse supernovae. RGB: Red giant branch stars. AGB: Asymptotic giant branch stars. J stars: J-type carbon stars.

abundances, sizes, and stellar sources. Figure 1 shows electron images of a selection of presolar grains. Nanodiamonds are the most abundant, but they are only ~ 2.5 nm in size (Figure 1d), so far precluding analysis of individual grains. Their presolar nature rests on the fact that they carry anomalous Xe and Te, but their average C isotopic ratio is normal (i.e., solar). Thus it cannot be ruled out that only a fraction of the diamonds have a stellar origin.

All other grain types are large enough that they can be analyzed as single grains for their isotopic compositions. Silicon carbide is the best studied grain type because almost pure SiC separates can be produced by chemical processing of meteorites and because trace element concentrations are high enough so that many elements can be analyzed in addition to C and Si. Essentially all SiC grains are of stellar origin. While average grain sizes are less than one μm , grains up to 50 μm have been found. Figure 1a shows an SEM image of an unusually large grain. Analysis in the ion microprobe has shown enormous ranges in the isotopic compositions of individual SiC grains and has led to the classification of different subtypes (see below).

The separation of graphite is more complicated than that of SiC.¹¹ Most presolar graphite grains are larger than 1 μm (Figure 1b,c) and can range up to 20 μm in size. They have been separated according to density, and grains of different density exhibit different isotopic signatures.¹¹ Many graphite grains contain tiny subgrains of titanium-, zirconium-, and molybdenum-rich carbides, cohenite (Fe_3C), kamacite (Fe-Ni), and elemental iron.^{12,13} These grains must have condensed before the graphite and in some cases apparently acted as condensation nuclei for graphite (Figure 1c).

The identification of presolar oxide and silicate grains is difficult. The reason is that the solar system is O-rich (i.e., has $\text{O} > \text{C}$), leading to the formation of O-rich minerals from isotopically homogenized material. These solar system silicates and oxides constitute a large background to O-rich stardust grains. Identification of presolar O-rich grains among this background requires isotopic measurements of individual grains in the ion microprobe (see below). Separation of oxide phases such as corundum (Al_2O_3), Mg spinel (MgAl_2O_4), and hibonite ($\text{CaAl}_{12}\text{O}_{19}$) by chemical processing still helps, because the fraction of presolar grains among these refractory phases is relatively high (1–2%).^{14,15} Some grains are larger than 1 μm (Figure 1e) and could be studied in detail.^{14,16}

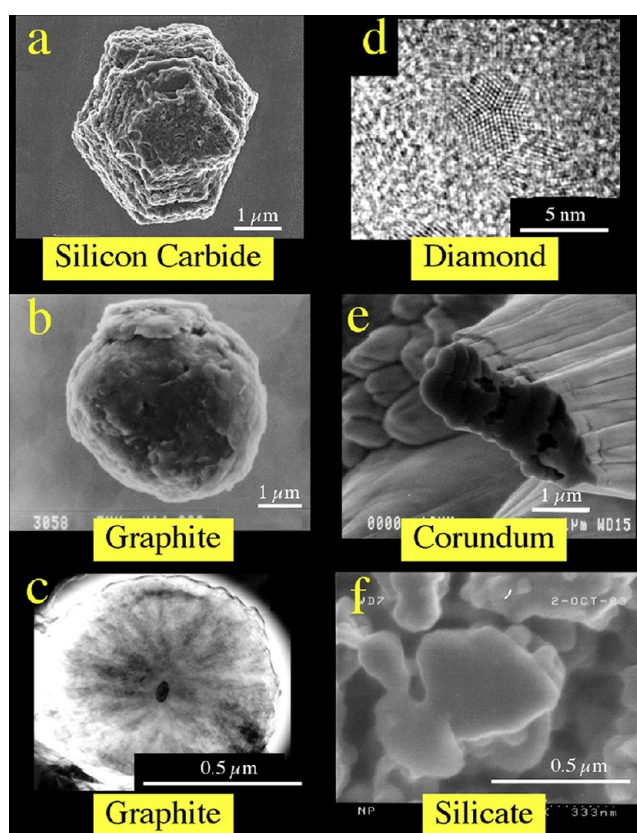


Figure 1. Secondary electron (a, b, e, f) and transmission electron (c, d) microscope images of presolar grains. (a) This large SiC grain shows euhedral features. (b) Graphite grain with smooth, shell-like surface (“onion type”). (c) Micrograph of a microtome slice of a presolar graphite grain. The TiC grain in the center of the graphite spherule apparently served as a condensation nucleus. (d) High-resolution TEM image of a diamond, showing its crystal structure. (e) Corundum (Al_2O_3) grain after some SIMS analysis. The primary ion beam sputtered the Au substrate the grain was located on. (f) The silicate grain in the center is a presolar grain as evidenced by its anomalous O isotopic ratios. Pictures courtesy of Sachiko Amari, Tom Bernatowicz, Tyrone Daulton, Scott Messenger, Ann Nguyen, and Larry Nittler.

Although silicates have the second-highest abundances, they have been discovered only recently because grains are smaller

than 1 μm and only one grain out of 5 000 grains is of presolar origin.^{17,18} Most of them are only 250–300 nm in size; the grain in Figure 1f is an exception.

ANALYTICAL TECHNIQUES AND GRAIN ANALYSIS

A whole plethora of analytical techniques has been applied to the analysis of stardust grains. These techniques probed their surface morphology, internal structure, and elemental and isotopic compositions. Measurements of isotopic ratios are most important because they provide information on the grains' stellar sources and nucleosynthetic processes therein, and by far most efforts have been devoted to them. Two basic types of isotopic analysis techniques have been applied, "bulk" analysis, the analysis of collections of large numbers of grains, and single grain analysis.

Isotopic Ratios. In spite of the low abundances of diamond, SiC, and graphite in meteorites, chemical and physical separation provides essentially pure samples with enough grains for bulk analysis. Bulk isotopic analysis has been performed by gas mass spectrometry for C, N, and the noble gases^{19,20} and by thermal ionization mass spectrometry (TIMS) for the heavy elements Sr, Ba, Nd, Sm, and Dy.²¹ Although only averages over many grains are obtained by these measurements, they make it possible to determine isotopic ratios of trace elements that cannot be obtained on single grains. Measurements can be done on grain size and density separates, and for gas MS by stepwise heating (pyrolysis) or combustion in an oxygen atmosphere. Analysis of the heavy noble gases in SiC samples has led to the conclusion that most of the grains come from Asymptotic Giant Branch (AGB) stars. This is based on the finding of s-process isotopic patterns in Kr and Xe.¹⁹ The s-process is the slow capture of neutrons where the density of neutrons is low enough that radioactive nuclides β -decay to stable nuclides before they can capture another neutron. This process takes place in AGB stars, stars that have evolved past the Red Giant Branch phase in their evolutionary sequence. These stars have burned all their H and He in the core and nuclear reactions take place in a thin layer between the core and the envelope.

If possible, measurements on single grains are preferred because correlated isotopic data of several elements from individual grains can serve to obtain the stellar origin of a given grain. The technique of choice is secondary ion mass spectrometry (SIMS) with the ion microprobe. Single grain analysis has revealed a tremendous range of isotopic ratios (see Figures 2 and 3). It also led to the identification of new grain types such as corundum (Al_2O_3)²² and spinel (MgAl_2O_4)¹⁴ and silicon nitride (Si_3N_4)²³ as well as of rare subpopulations of SiC grains.²⁴ While most isotopic measurements up to the year 2000 have been made on $>1 \mu\text{m}$ grains, a new type of ion microprobe, the NanoSIMS, allows analysis of grains down to 100 nm in size. The NanoSIMS was instrumental in the discovery of presolar silicates in interplanetary dust particles¹⁷ and primitive meteorites.¹⁸ For isotopic measurement, grains from residues (SiC, graphite, oxides) are usually deposited on a gold substrate from suspension, so that they are well separated from one another, and ion microprobe measurements are made by focusing the primary ion beam onto individual grains. In this way, more than 10 000 single SiC grains and more than 1 000 graphite grains have been analyzed for their isotopic ratios.²⁵ These measurements can be made not only on the major elements but also on minor and trace elements such as N, Mg, K, Ca, Ti, Fe, and Ni.

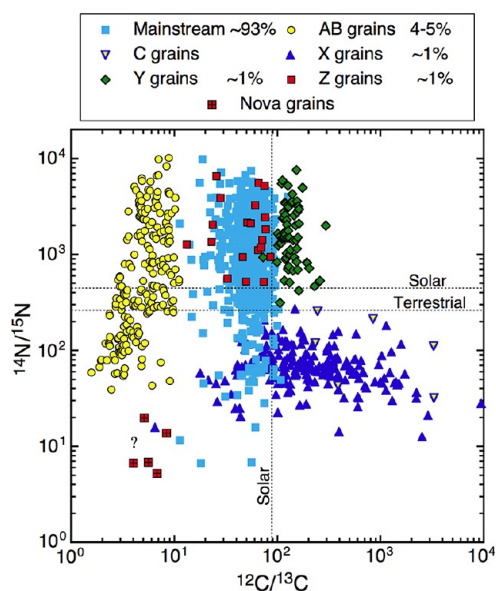


Figure 2. Nitrogen and carbon isotopic ratios of individual presolar SiC grains. Because rare grain types have been identified by special automatic imaging searches, the number of grains of different types do not correspond to their relative abundances in meteorites. These abundances are given in the legend. The dotted lines indicate the solar (terrestrial) isotopic ratios.

Figures 2 and 3 show the C, N, and Si isotopic ratio measured in individual SiC grains. These grains are classified based on their isotopic compositions, and these compositions are used to infer stellar sources. Two main stellar sources of SiC grains could be identified: AGB stars and core-collapse supernovae. Mainstream grains are from low-mass (1.5–3 solar masses) AGB star of close-to-solar metallicity (metallicity is the abundance of "metals", all elements heavier than He.) Grains of type Y and Z seem to come from AGB stars with lower-than-solar metallicities. SiC X grains come from supernovae, massive stars (>10 solar masses) that end their lives in gigantic explosions. Evidence comes from ^{28}Si excesses, in some grains also from the initial presence of ^{44}Ti (from large ^{44}Ca excesses). Titanium-44 is a radioisotope with a half-life of 60 years, which decays into ^{44}Ca . Both ^{28}Si and ^{44}Ti are only produced in massive stars. Although type C grains have ^{29}Si and ^{30}Si excesses, they also have a SN origin. Grains of type AB are probably from J stars and/or from post-AGB stars that have undergone a very late thermal pulse (explosive burning of the He shell), and a few grains appear to have an origin in novae (a star in a binary system undergoing explosive H burning on the surface). Silicon nitride grains are found in SiC-rich residues. They are extremely rare and have the isotopic signatures of SiC X grains, thus have a SN origin.

Rare grain types are located by automatic imaging searches where images of the Au foil carrying the grains in selected isotopes are used to identify grains of interest that are subsequently analyzed in detail. In ion microprobes with direct imaging capabilities (e.g., the Cameca IMS instruments), direct images are used. In the NanoSIMS, images are obtained by rastering the primary ion beam over the sample surface and detecting secondary ions as a function of position. This instrument can detect up to 7 isotopes simultaneously. Automatic isotopic imaging has played an important role in the discovery of presolar silicates. Presolar silicates are small (typically 250–300 nm in diameter) and have to be detected in

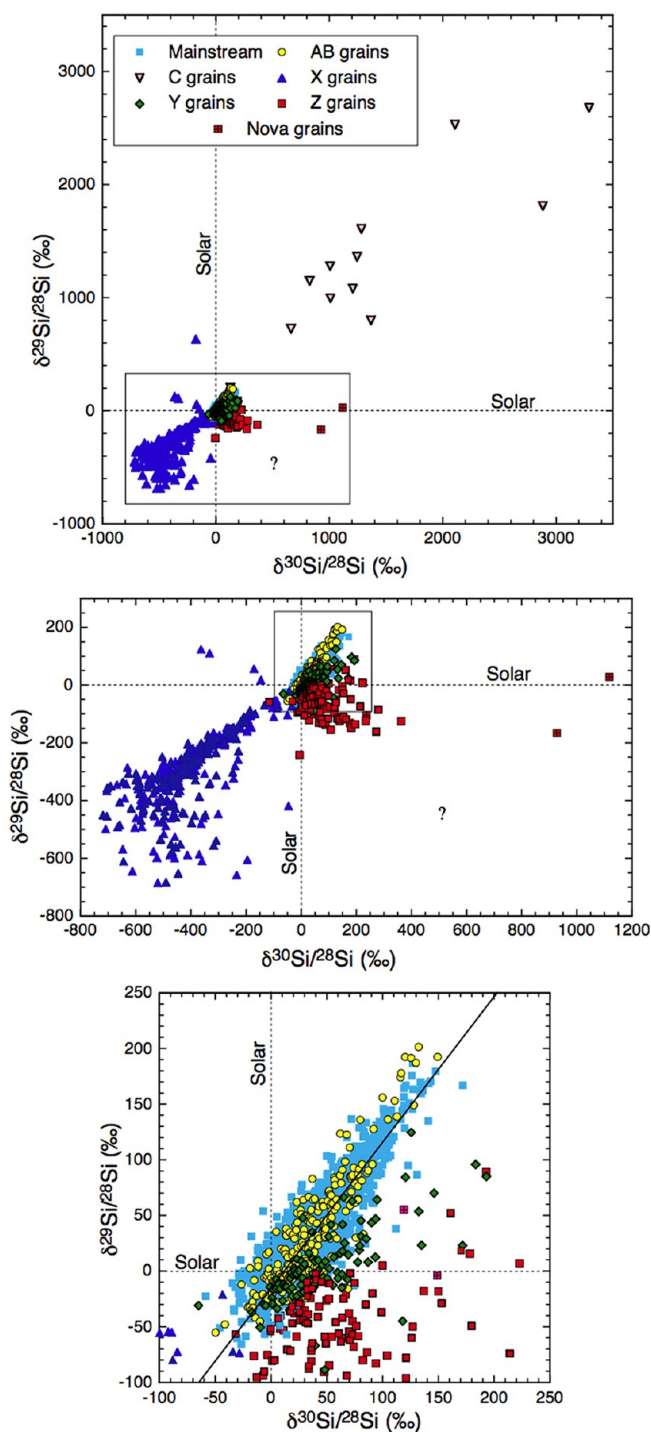


Figure 3. Silicon isotopic ratios of presolar SiC grains. Ratios are plotted as δ -values, deviations from the solar (terrestrial) ratios in parts per thousand (permil, ‰).

the presence of an overwhelming number of isotopically normal silicates of solar system origin. This makes it necessary to measure the isotopic compositions of thousands and ten thousands grains. Figure 4 shows O-isotopic ratio images of a $10\ \mu\text{m} \times 10\ \mu\text{m}$ area densely covered with small grains from the Acfer 094 primitive meteorite.¹⁸ One grain is identified by its anomalous isotopic compositions (excess of ^{17}O and deficit in ^{18}O). Mg-oxide and Si images are also shown, identifying the grain as a Mg-rich silicate. Isotopic imaging searches of tightly

packed grain separates and polished meteorite sections to date have identified more than 500 presolar silicate grains.²⁵

Laser ablation and resonant ionization mass spectrometry (RIMS) has been applied to the isotopic analysis of the heavy elements Sr, Zr, Mo, Ru, and Ba in single presolar SiC and graphite grains.^{26–28} This technique uses laser beams of finely tuned wavelengths to selectively ionize the neutral atoms of a given element sputtered from the sample by an ion beam or desorbed by a laser pulse. Its unique advantage is the fact that a chosen element can be ionized selectively at the exclusion of any isobaric interferences. Thus it is possible to measure Zr isotopes in the presence of Mo and vice versa. These elements have isobars at the same atomic masses. Another advantage is that a relatively high proportion of atoms can be ionized, increasing sensitivity and making the analysis of low-abundance elements possible. An important RIMS result is the identification of the initial presence of ^{99}Tc (half live 2.1×10^5 years) in presolar SiC grains.²⁸ The detection of Tc, which does not have any stable isotopes, in stars played an important role in the history of the theory of nucleosynthesis.¹ To date, all RIMS analyses of presolar grains have been made with a single instrument at Argonne National Laboratory. A new RIMS instrument at the University of Chicago will lead to increased stardust studies by this technique.

Another technique that allows isotopic analysis on single grains is laser heating and gas MS of noble gases.²⁹ Helium and Ne measurements have been made on presolar SiC and graphite grains,^{30,31} allowing, for example, the determination of interstellar residence times of SiC grains from ^{21}Ne produced by galactic cosmic rays.

Finally, a promising technique for isotopic analysis on tiny samples is atom probe tomography. This technique combines emission of ions from a small tip and time-of-flight MS and allows the determination of mass and position of individual atoms in a sample with 50% efficiency.³² The average $^{12}\text{C}/^{13}\text{C}$ ratio of nanodiamonds is terrestrial (89). Although a diamond contains only ~ 2000 atoms, there is hope that the atom probe will make it possible to determine whether individual nanodiamonds all have the same or a range of isotopic compositions.³³

Elemental Abundances. In addition to isotopic ratios, the ion microprobe can be used to determine elemental abundances in stardust grains.³⁴ There are several other techniques that allow the measurement of element contents. Energy-dispersive X-ray (EDX) analysis in the SEM has been applied to presolar grains to identify different mineral phases on a grain mount before SIMS analysis on selected grains. Because the Si concentration in SiC is higher than in silicates, X-ray imaging in the SEM has been used to detect presolar SiC grains in polished sections of a meteorite.³⁵

EDX analysis has also been used in the transmission electron microscope (TEM) to determine concentrations of minor elements in presolar grains.³⁶ The finding of Mo/Ti ratios much higher than the solar system ratio in TiC subgrains within graphite spherules has led to the conclusion that the grains had an AGB origin.³⁷ Molybdenum is an s-process element, and AGB stars produce such elements in overabundance. Samples for TEM analysis are usually microtome sections of presolar grains. This works best for graphite grains,^{12,13} but microtome sections of SiC have also been analyzed.³⁶ Preparation by focused ion beam (FIB) microscopy is preferred for very small grains,³⁸ for example, silicate grains identified by NanoSIMS isotopic imaging.^{39,40}

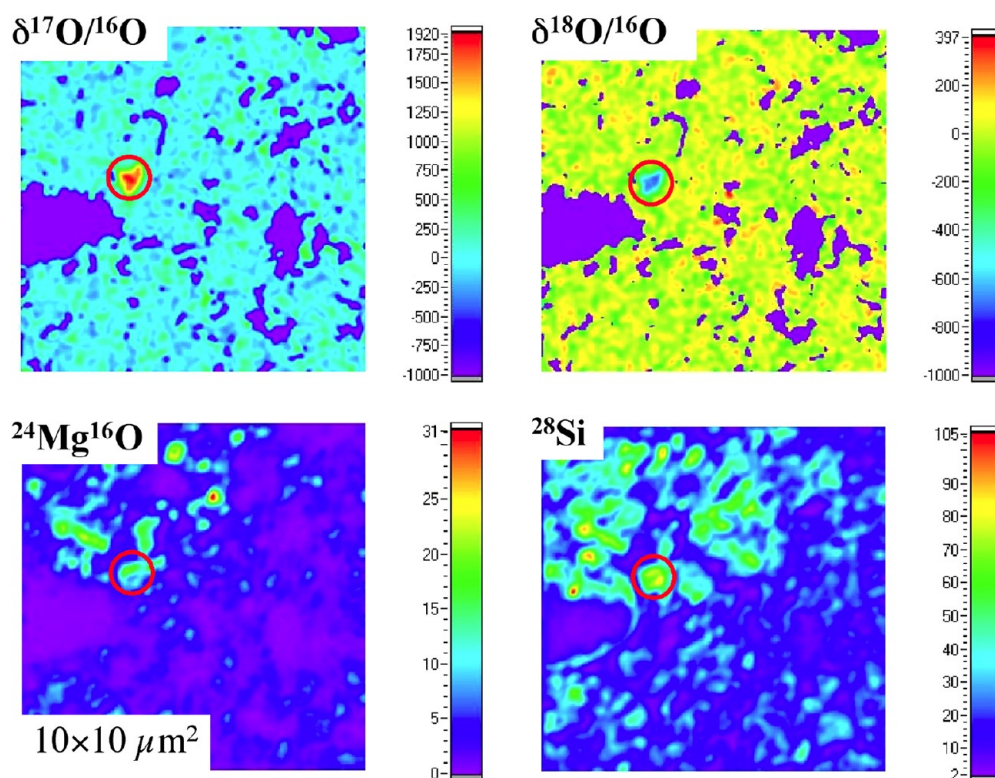


Figure 4. Oxygen isotopic ratio images obtained from NanoSIMS images of tightly packed grains from a primitive meteorite. Isotopic ratios are shown as δ -values, deviations from the solar (terrestrial) ratios in parts per thousand (permil, ‰). One grain has anomalous O isotopic ratios, an excess in ^{17}O and a deficit in ^{18}O relative to solar ratios. Also shown are MgO and Si images. These images identify the anomalous grain as a Mg-rich silicate. An enlarged SEM micrograph of the presolar silicate identified from these isotopic images (encircled) is shown in Figure 1f. Figure modified with permission from ref 18. Copyright 2004 American Association for the Advancement of Science.

The Auger Nanoprobe uses the characteristic energy of Auger electrons to obtain chemical and mineralogical information of submicrometer samples. Because Auger electrons are detected only from the top few nanometers, Auger microscopy avoids the problem of the large volume from which X-rays are emitted. This makes it the ideal complement of the NanoSIMS for in situ elemental analysis of presolar grains identified by isotopic ion imaging.^{41,42}

Synchrotron X-ray fluorescence (XRF) uses characteristic X-rays produced by a (usually) monochromatic finely focused X-ray beam. Because of the atomic charge dependence of fluorescence, it is best suited to the analysis of heavy elements. Element images can be obtained by raster scanning. It has been successfully applied to the analysis of trace elements in presolar SiC grains $\sim 2 \mu\text{m}$ in size, providing evidence for the condensation of short-lived ^{93}Zr (half-life of 1.5×10^6 years) into the grains at the time of their formation.⁴³

Structural Studies. The crystal structure and the internal composition of presolar grains can provide information about the chemical and physical conditions under which the grains formed.⁴⁴ A variety of techniques has been applied to structural studies of presolar grains. Imaging in the SEM reveals the surface morphology of grains. Such studies of “pristine” SiC grains, which were extracted from the meteorite without destructive chemical treatment, revealed crystal features consisted with the cubic (3C) polytype of SiC.⁴⁵ On the basis of SEM images, presolar graphite grains were divided into two basic morphology types: “onions” and “cauliflowers”.⁴⁶ The first are spheres with smooth or shell-like platy surfaces and are preferentially found among high-density grains; the latter

consist of dense aggregates of small scales and are prevalent among low-density grains.

Raman spectroscopy was instrumental in the discovery of presolar SiC.³ Raman microprobe analysis has been successfully applied to individual SiC grains⁴⁷ and presolar graphite grains.^{48,49} The latter study could determine the degree of crystallinity and confirmed the morphological observations: high-density grains are on average better crystallized than low-density grains.

TEM studies have shown that presolar graphite grains contain small (20–500 nm) subgrains.^{13,50} Most of these subgrains are TiC, but kamacite (Fe–Ni), cohenite (Fe_3C), rutile (TiO_2), SiC, and Fe grains have also been found.^{51,52} Selected area electron diffraction (SAED) in the TEM has been used to determine the crystal structure of presolar SiC grains.⁵³ It was found that the only polytypes are the cubic 3C (β -SiC) and the hexagonal 2H (α -SiC), and intergrowths between the two. SAED was also instrumental in confirming the mineralogy of various subgrains.^{13,50–52} TEM imaging studies found that the surface morphology of graphite grains is reflected in their internal structure.^{12,50} Cauliflowers consist of concentrically packed scales of poorly crystallized and turbostratic carbon, whereas onions either consist of well-crystallized graphite throughout (Figure 1c shows an example) or of a mantle of well-crystallized graphite and a core of tightly packed graphene sheets. The structure of these cores was probed by electron energy loss spectroscopy (EELS), which can give information on the nature of carbon bonds. It can also reveal the mineralogy of subgrains.⁵⁴ High-resolution TEM has been used for determining the lattice structure of nanodiamonds.⁵⁵ Figure

Id shows an example. Studies with aberration-corrected scanning TEM with single-atom sensitivity showed that meteoritic nanodiamond residues contain two phases of carbon: crystalline nanodiamonds and glassy carbon, a disordered phase with sp^2 bonding.⁵⁶

TEM studies of two Al_2O_3 grains with an AGB star origin revealed one to be crystalline (corundum) and the other amorphous, indicating that AGB stars can produce both phases.⁵⁷ Both crystalline and amorphous grains were also found among presolar silicates; when crystalline, grains tend to be olivine.^{40,58} TEM analysis led to the identification of a new mineral, $MgSiO_3$ perovskite, previously not found among presolar grains.³⁹

A couple of techniques using synchrotron X-ray beams are still in their infancy as far as application to presolar grains is concerned. One is X-ray absorption near edge structure (XANES).⁵⁴ Similar to EELS, it can be used to determine the oxidation state of Fe and Ti and the nature of carbon bonds. Another one is X-ray computed microtomography (XRCMT), which combines several XRF images to obtain the three-dimensional distribution of elements within a small object. Analysis of a presolar graphite grain shows the distribution of internal TiC subgrains.⁵⁹ Wide-angle X-ray scattering (WAXS) analysis of the same grains shows the orientation of the crystalline parts of the grain. It is hoped that these techniques will find increasing use for analyzing the structure of presolar grains in the future.

CONCLUSIONS

The study of stardust grains in the laboratory has become a new branch of astronomy. The grains provide information on isotopic ratios that could not be obtained from stars. Of special interest are results that do not agree with stellar models⁶⁰ and thus trigger the refinement of those stellar models, the measurement of cross sections,⁶¹ or the search for new processes not considered before. The field is vigorously expanding, and technical advances are expected to yield new surprises.

AUTHOR INFORMATION

Corresponding Author

*E-mail: ekz@wustl.edu.

Notes

The author declares no competing financial interest.

Biography

Ernst Zinner is Research Professor of Physics and Earth and Planetary Sciences at Washington University in St. Louis. For 40 years he has been involved in the laboratory analysis of lunar rocks, meteorites, and interplanetary dust. For the last 25 years he has concentrated on the study of stardust, dust grains from other stars. For this work he has been called "Lithic Astronomer."

REFERENCES

- (1) Burbidge, E. M.; Burbidge, G. R.; Fowler, W. A.; Hoyle, F. *Rev. Mod. Phys.* **1957**, *29*, 547–650.
- (2) Cameron, A. G. W. *Publ. Astron. Soc. Pacific* **1957**, *69*, 201–222.
- (3) Bernatowicz, T.; Fraundorf, G.; Tang, M.; Anders, E.; Wopenka, B.; Zinner, E.; Fraundorf, P. *Nature* **1987**, *330*, 728–730.
- (4) Lewis, R. S.; Tang, M.; Wacker, J. F.; Anders, E.; Steel, E. *Nature* **1987**, *326*, 160–162.
- (5) Clayton, D. D.; Nittler, L. R. *Ann. Rev. Astron. Astrophys.* **2004**, *42*, 39–78.
- (6) Lodders, K.; Amari, S. *Chem. Erde* **2005**, *65*, 93–166.

- (7) Zinner, E. In *Treatise on Geochemistry Update*; Holland, H. D., Turekian, K. K., Davis, A., Eds.; Elsevier Ltd.: Oxford, U.K., 2007; Vol. 1.02 (online update only), pp 1–33.
- (8) Clayton, R. N.; Grossman, L.; Mayeda, T. K. *Science* **1973**, *182*, 485–488.
- (9) Anders, E.; Zinner, E. *Meteoritics* **1993**, *28*, 490–514.
- (10) Amari, S.; Anders, E.; Virag, A.; Zinner, E. *Nature* **1990**, *345*, 238–240.
- (11) Amari, S.; Lewis, R. S.; Anders, E. *Geochim. Cosmochim. Acta* **1994**, *58*, 459–470.
- (12) Bernatowicz, T. J.; Cowsik, R.; Gibbons, P. C.; Lodders, K.; Fegley, B., Jr.; Amari, S.; Lewis, R. S. *Astrophys. J.* **1996**, *472*, 760–782.
- (13) Croat, T. K.; Bernatowicz, T.; Amari, S.; Messenger, S.; Stadermann, F. J. *Geochim. Cosmochim. Acta* **2003**, *67*, 4705–4725.
- (14) Nittler, L. R.; Alexander, C. M. O. D.; Gao, X.; Walker, R. M.; Zinner, E. *Astrophys. J.* **1997**, *483*, 475–495.
- (15) Zinner, E.; Amari, S.; Guinness, R.; Nguyen, A.; Stadermann, F.; Walker, R. M.; Lewis, R. S. *Geochim. Cosmochim. Acta* **2003**, *67*, 5083–5095.
- (16) Nittler, L. R.; Alexander, C. M. O. D.; Gallino, R.; Hoppe, P.; Nguyen, A. N.; Stadermann, F. J.; Zinner, E. *Astrophys. J.* **2008**, *682*, 1450–1478.
- (17) Messenger, S.; Keller, L. P.; Stadermann, F. J.; Walker, R. M.; Zinner, E. *Science* **2003**, *300*, 105–108.
- (18) Nguyen, A. N.; Zinner, E. *Science* **2004**, *303*, 1496–1499.
- (19) Lewis, R. S.; Amari, S.; Anders, E. *Geochim. Cosmochim. Acta* **1994**, *58*, 471–494.
- (20) Amari, S.; Lewis, R. S.; Anders, E. *Geochim. Cosmochim. Acta* **1995**, *59*, 1411–1426.
- (21) Hoppe, P.; Ott, U. In *Astrophysical Implications of the Laboratory Study of Presolar Materials*; Bernatowicz, T. J., Zinner, E., Eds.; AIP: New York, 1997; pp 27–58.
- (22) Nittler, L. R.; Alexander, C. M. O. D.; Gao, X.; Walker, R. M.; Zinner, E. *Nature* **1994**, *370*, 443–446.
- (23) Nittler, L. R.; Hoppe, P.; Alexander, C. M. O. D.; Amari, S.; Eberhardt, P.; Gao, X.; Lewis, R. S.; Strebler, R.; Walker, R. M.; Zinner, E. *Astrophys. J.* **1995**, *453*, L25–L28.
- (24) Amari, S.; Hoppe, P.; Zinner, E.; Lewis, R. S. *Astrophys. J.* **1992**, *394*, L43–L46.
- (25) Hynes, K. M.; Gyngard, F. *Lunar Planet. Sci.* **2009**, *XL*; abstract no. 1198.
- (26) Nicolussi, G. K.; Pellin, M. J.; Lewis, R. S.; Davis, A. M.; Clayton, R. N.; Amari, S. *Astrophys. J.* **1998**, *504*, 492–499.
- (27) Lugaro, M.; Davis, A. M.; Gallino, R.; Pellin, M. J.; Straniero, O.; Käppeler, F. *Astrophys. J.* **2003**, *593*, 486–508.
- (28) Savina, M. R.; Davis, A. M.; Tripa, C. E.; Pellin, M. J.; Gallino, R.; Lewis, R. S.; Amari, S. *Science* **2004**, *303*, 649–652.
- (29) Nichols, R. H., Jr.; Kehm, K.; Hohenberg, C. M. In *Advances in Analytical Geochemistry*; Hyman, M., Rowe, M., Eds.; JAI Press Inc.: Greenwich, CT, 1995; Vol. 2, pp 119–140.
- (30) Heck, P. R.; Gyngard, F.; Ott, U.; Meier, M. M. M.; Avila, J. N.; Amari, S.; Zinner, E.; Lewis, R. S.; Baur, H.; Wieler, R. *Astrophys. J.* **2009**, *698*, 1155–1164.
- (31) Heck, P. R.; Amari, S.; Hoppe, P.; Baur, H.; Lewis, R. S.; Wieler, R. *Astrophys. J.* **2009**, *701*, 1415–1425.
- (32) Kelly, T. F.; Miller, M. K. *Rev. Sci. Instrum.* **2007**, *78*, 031101–031101-20.
- (33) Heck, P. R.; Pellin, M. J.; Davis, A. M.; Isheim, D.; Seidman, D. N.; Hillier, J.; Mane, A.; Elam, J.; Savina, M. R.; Auciello, O.; Stephan, T.; Larson, D. J.; Lewis, J.; Floss, C.; Daulton, T. L. *Lunar Planet. Sci.* **2012**, *XLIII*, abstract no. 1790.
- (34) Amari, S.; Hoppe, P.; Zinner, E.; Lewis, R. S. *Meteoritics* **1995**, *30*, 679–693.
- (35) Alexander, C. M. O. D.; Swan, P.; Walker, R. M. *Nature* **1990**, *348*, 715–717.
- (36) Hynes, K. M.; Croat, T. K.; Amari, S.; Mertz, A. F.; Bernatowicz, T. J. *Meteorit. Planet. Sci.* **2010**, *45*, 596–614.
- (37) Croat, T. K.; Stadermann, F. J.; Bernatowicz, T. J. *Astrophys. J.* **2005**, *631*, 976–987.

- (38) Holzapfel, C.; Soldera, F.; Vollmer, C.; Hoppe, P.; Mücklich, F. *J. Microsc.* **2009**, *235*, 59–66.
- (39) Vollmer, C.; Hoppe, P.; Brenker, F. E.; Holzapfel, C. *Astrophys. J.* **2007**, *666*, L49–L52.
- (40) Vollmer, C.; Brenker, F. E.; Hoppe, P.; Stroud, R. *Astrophys. J.* **2009**, *700*, 774–782.
- (41) Stadermann, F. J.; Floss, C.; Bose, M.; Lea, A. S. *Meteorit. Planet. Sci.* **2009**, *44*, 1033–1049.
- (42) Floss, C.; Stadermann, F. *Geochim. Cosmochim. Acta* **2009**, *73*, 2415–2440.
- (43) Kashiv, Y.; Davis, A. M.; Gallino, R.; Cai, Z.; Lai, B.; Sutton, S. R.; Clayton, R. N. *Astrophys. J.* **2010**, *713*, 212–219.
- (44) Bernatowicz, T. J.; Akande, O. W.; Croat, T. K.; Cowsik, R. *Astrophys. J.* **2005**, *631*, 988–1000.
- (45) Bernatowicz, T. J.; Messenger, S.; Pravdivtseva, O.; Swan, P.; Walker, R. M. *Geochim. Cosmochim. Acta* **2003**, *67*, 4679–4691.
- (46) Hoppe, P.; Amari, S.; Zinner, E.; Lewis, R. S. *Geochim. Cosmochim. Acta* **1995**, *59*, 4029–4056.
- (47) Wopenka, B.; Jadhav, M.; Lebsack, E.; Zinner, E. *Lunar Planet. Sci.* **2010**, *XL1*, abstract no. 1390.
- (48) Wopenka, B.; Jadhav, M.; Zinner, E. *Lunar Planet. Sci.* **2011**, *XLII*, abstract no. 1162.
- (49) Wopenka, B.; Groopman, E.; Zinner, E. *Meteorit. Planet. Sci.* **2011**, *46*, A252.
- (50) Bernatowicz, T. J.; Amari, S.; Zinner, E. K.; Lewis, R. S. *Astrophys. J.* **1991**, *373*, L73–L76.
- (51) Croat, T. K.; Stadermann, F. J.; Bernatowicz, T. J. *Astron. J.* **2010**, *139*, 2159–2169.
- (52) Croat, T. K.; Jadhav, M.; Lebsack, E.; Bernatowicz, T. *Lunar Planet. Sci.* **2011**, *XLII*, abstract no. 1533.
- (53) Daulton, T. L.; Bernatowicz, T. J.; Lewis, R. S.; Messenger, S.; Stadermann, F. J.; Amari, S. *Geochim. Cosmochim. Acta* **2003**, *67*, 4743–4767.
- (54) Groopman, E. E.; Daulton, T. L.; Nittler, L. R.; Bernatowicz, T. J.; Zinner, E. K. *Meteorit. Planet. Sci.* **2012**, *47*, abstract no. 5225.
- (55) Daulton, T. L.; Eisenhour, D. D.; Bernatowicz, T. J.; Lewis, R. S.; Buseck, P. R. *Geochim. Cosmochim. Acta* **1996**, *60*, 4853–4872.
- (56) Stroud, R. M.; Chisholm, M. F.; Heck, P. R.; Alexander, C. M. O. D.; Nittler, L. R. *Astrophys. J.* **2011**, *738*, L27 (25pp).
- (57) Stroud, R. M.; Nittler, L. R.; Alexander, C. M. O. D. *Science* **2004**, *305*, 1455–1457.
- (58) Messenger, S.; Keller, L. P.; Lauretta, D. S. *Science* **2005**, *309*, 737–741.
- (59) Schmitz, S.; Brenker, F. E.; Schmitt, M.; Vekemans, B.; Vincze, L.; Schoonjans, T.; Wellenreuther, G.; De Samber, B.; Falkenberg, G.; Burghammer, M.; Jadhav, M. *Meteorit. Planet. Sci.* **2012**, *47*, abstract no. 5215.
- (60) Lin, Y.; Gyngard, F.; Zinner, E. *Astrophys. J.* **2010**, *709*, 1157–1173.
- (61) Koehler, P. E.; Spencer, R. R.; Guber, K. H.; Winters, R. R.; Raman, S.; Harvey, J. A.; Hill, N. W.; Blackmon, J. C.; Bardayan, D. W.; Larson, D. C.; Lewis, T. A.; Pierce, D. E.; Smith, M. S. *Phys. Rev. C* **1998**, *57*, R1558–R1561.